Manchester Metropolitan University

e-space

Manchester Metropolitan University's Research Repository

Please cite the Published Version

George, Jeena, Uko, Mfonobong, Ekpo, Sunday, Ijaz, Muhammad, Kharel, Rupak, Wang, Qiuyu and Ji, Helen (2020) Design of a Multiband RF Slotted-Antenna for Biosensing Applications. In: 12th IEEE/IET International Symposium on Communication Systems, Networks and Digital Signal Processing Conference, 20 July 2020 - 22 July 2020, Porto, Portugal.

DOI: https://doi.org/10.1109/CSNDSP49049.2020.9249616

Publisher: IEEE

Version: Accepted Version

Downloaded from: https://e-space.mmu.ac.uk/630106/

Usage rights: © In Copyright

Additional Information: © 2020 IEEE. Personal use of this material is permitted. Permission from IEEE must be obtained for all other uses, in any current or future media, including reprinting/republishing this material for advertising or promotional purposes, creating new collective works, for resale or redistribution to servers or lists, or reuse of any copyrighted component of this work in other works.

Enquiries:
If you have questions about this document, contact openresearch@mmu.ac.uk. Please include the URL of the record in e-space. If you believe that your, or a third party's rights have been compromised through this document please see our Take Down policy (available from https://www.mmu.ac.uk/library/using-the-library/policies-and-guidelines)

Design of a Multiband RF Slotted-Antenna for Biosensing Applications

Jeena George
Faculty of Science and Engineering
Manchester Metropolitan University
Manchester, United Kingdom
jeenageorge94@gmail.com

Mfonobong C. Uko
Faculty of Science and Engineering
Manchester Metropolitan University
Manchester, United Kingdom
mfonobong.uko@stu.mmu.ac.uk

Sunday C. Ekpo
Faculty of Science and Engineering
Manchester Metropolitan University
Manchester, United Kingdom
s.ekpo@mmu.ac.uk

Muhammed Ijaz
Faculty of Science and Engineering
Manchester Metropolitan University
Manchester, United Kingdom
M.Ijaz@mmu.ac.uk

Rupak Kharel
Faculty of Science and Engineering
Manchester Metropolitan University
Manchester, United Kingdom
r.kharel@mmu.ac.uk

Qiuyu Wang
Faculty of Science and Engineering
Manchester Metropolitan University
Manchester, United Kingdom
Q.Wang@mmu.ac.uk

Helen Ji
Faculty of Science and Engineering
Manchester Metropolitan University
Manchester, United Kingdom
h.ji@mmu.ac.uk

***Abstract*—There is an expanding demand for adaptive contactless label-free biosensors for point-of-care, multi-user, health risk-free applications. This paper introduces the design of an elliptically-slotted patch antenna (ESPA) for bio-sensing applications. The resonance frequency difference of the ESPA is 2.5% compared with the basic slot-less patch antenna of 6.6%. Hence, the proposed model compares with the conventional slot-less patch antenna and exhibited a vast improvement in its bandwidth efficiency by over 62%. The simulated ESPA design yields a total gain of 7.5 dBi and can be utilized for simultaneous bio-sample detection and signal transmission applications.**

***Keywords*—5G, Biomedical Sensors, Multi-band, Passive biosensor patch antenna.**

I. INTRODUCTION

The utilization of radio waves and intense magnetic fields to identify the variation in the energy absorption rate resulted in the development of the magnetic resonance imaging (MRI) technique. This method creates better quality pictures with the introduction of contrast liquid into breast tissues and is excellent at late-stage diagnosis of cancer cells. However, this procedure is highly expensive and takes long screening time for the detection of tumours. [1], [2], [3], [4].

Microwave-based breast imaging methods are favoured by the patients as they are safer due to non-ionizing radiation. The electrical properties such as permittivity and conductivity variation in each tissue depend on the water content in it. This property is exploited to detect the presence of tumours from the healthy host tissue as malignant tissues possess more water and thereby higher permittivity than other tissues [5].

Several studies in literature proved lower values of permittivity and conductivity for fatty tissues and higher values for the glandular tissues with the breast tissue. The potential of microwaves to detect the existence of small malignant tissues in a rapid, sensitive and specific way is possible with the assistance of its electrical property variations [6].

The return loss (S11) and the dielectric properties corresponding to each biotic specimen varies under RF/microwave frequencies and this feature is exploited by antenna biosensors for sensing. The development of devices with compact size makes it more convenient to deal with remote advanced radio access technologies (e.g. 5G) and network communications [7], [8], [9]. The potential of the novel elliptically-slotted patch antenna (ESPA) system can be stretched to space-based bio-sensing devices by incorporating the vast opportunities in wireless communication [10], [11], [12], [13].

This paper is organized as follows. Section II presents the patch antenna system design including the system design parameters, the system model of the elliptically-slotted patch antenna and further order configurations. In section III, the simulation parameters, results and discussion are stated. The paper is concluded in section IV.

II. PATCH ANTENNA SYSTEM DESIGN

The model of the novel patch antenna system is created using a computational electromagnetic software product called FEKO with an elliptical slot on it and shown in Fig. 1. The elliptical slot is designed at the centre of the patch to detect the variations in the performance of the antenna with the introduction of a biological sample in it.

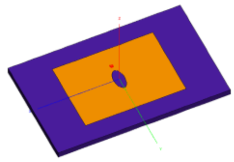

Fig. 1. ESPA System on Finite Ground

The second-order model is created and Fig. 2 shows the front view of its CAD model. Fig. 3 and Fig. 4 shows third-order configurations with various positioning of the ellipses. However, the second method of third-order ESPA designed such a way that three ellipses joined together towards the centre of the patch.

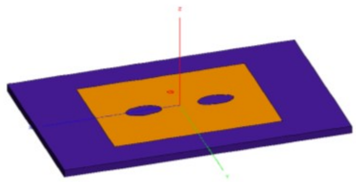

Fig. 2. Second-Order ESPA System Model

Fig. 5 shows the fourth-order ESPA with four ellipses on the patch with a distance of 20 mm and 14 mm between the centres of ellipses horizontally and vertically respectively.

III. RESULT AND DISCUSSION

A. Performance of CSPA versus ESPA

The outstanding potential of electronic technologies exerted into the biotic field to understand the physiological variations in the body and ultimately leads to the development of biosensors. The active sensing part that acts as a biosensor in this investigation is the patch antenna and the performance

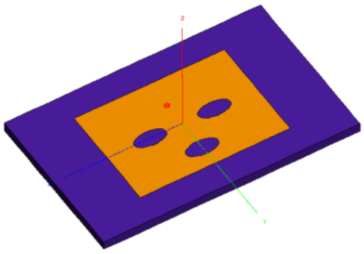

Fig. 3. Third-Order ESPA System Model

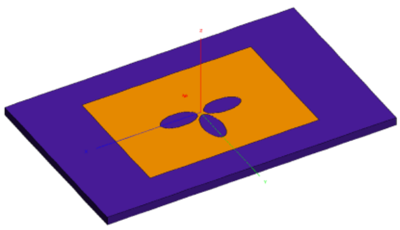

Fig. 4. Third-Order ESPA System Model (Closer Approach)

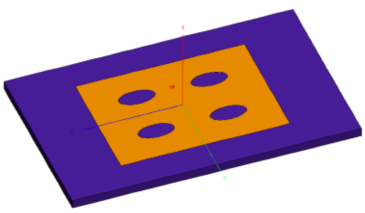

Fig. 5. Fourth-Order ESPA System Mode

of conventional slot-less patch antenna (CSPA) is compared with the elliptically slotted patch antenna (ESPA). The operating frequency of the model is selected as 2.79 GHz with a frequency range of 2.6 GHz and 3.0 GHz. The design specifications of this first order ESPA model is in Table I.

TABLE I

Model Parameters Parameter	Value (mm)
Patch Width	46.8
Patch Depth	33.2
Substrate Height	2.87
Substrate Width	80
Substrate Depth	50
Feed Distance	8.9
Feed Radius	0.65
Minor Radius of Ellipse	2.5
Major Radius of Ellipse	5

The models of both antenna systems are created and the performance is analysed on finite and infinite grounds. The infinite system designed such that the ground is a planar multilayer substrate with layer 1 as a perfect electric conductor (PEC) with a thickness of substrate height whereas, homogeneous free space medium is considered for finite ground design. Fig. 6 and Fig. 7 give the reflection coefficient versus frequency for CSPA and ESPA systems respectively.

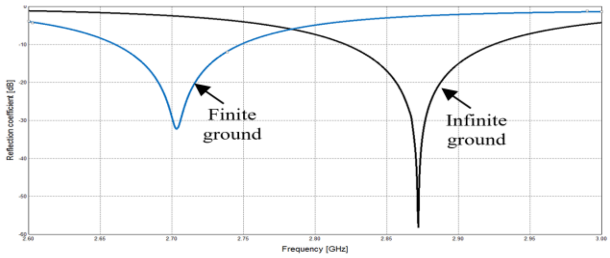

Fig. 6. Reflection Coefficient versus Frequency (CSPA)

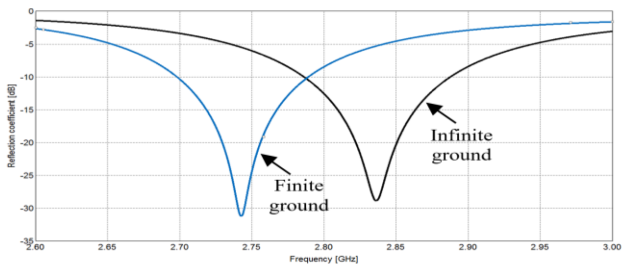

Fig. 7. Reflection Coefficient versus Frequency (ESPA)

The resonating frequencies of CSPA on the infinite ground are about 2.87 GHz and 2.70 GHz on the finite ground. This conventional patch antenna system introduces a general difference of 5.9% in its resonance frequency. However, the designed ESPA model resonates at 2.83 GHz on the infinite ground and at 2.74 GHz on the finite ground with a resonance frequency difference of about 3.1%. A considerable improvement of almost 2.8% of the CSPA model is achieved using the proposed design. Any sensor design based on electromagnetic principles should exhibit an acceptable interrelationship with simulated and real-life models. The concurrence of reflection coefficient values on infinite and finite grounds of CSPA is approximately -6.0 dB (Fig. 6) whereas, it is much better in ESPA with -11.0 dB (Fig. 7) at the operating frequencies.

The geometrical size of the ESPA system modulated such that it emulates with the infinite estimation as the practical implementation follows the simulated designs. The system is flexible in terms of its weight, portability and even allows the merging of designs based on meta-materials which improves the bio-sensing capabilities. The impedance magnitude and voltage standing wave ratio (VSWR) of the ESPA system are shown in Fig. 8 and Fig. 9. In any given RF design, there is a factor that opposes the designed system known as impedance and the proposed ESPA model achieved a characteristic impedance of 50 at a frequency of 2.74 GHz.

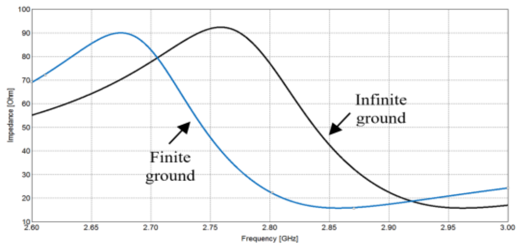

Fig. 8. Impedance Magnitude of the ESPA System

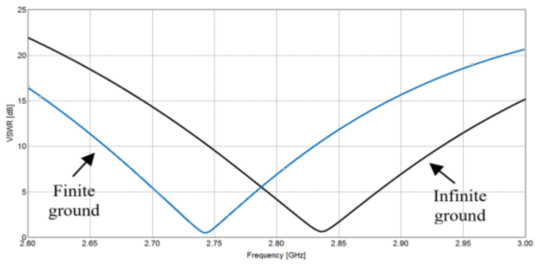

Fig. 9. VSWR of the ESPA System

In order to improve the power transmission from the source to load, an impedance matching circuit is a crucial criterion in bio-sensing designing. Such a system leads to a balanced system with less deformed signals in bio-sensing applications. The VSWR values of the infinite and finite models are about 1 dB at 2.74 GHz and 2.83 GHz respectively. Fig. 10 depicts the radiation pattern of the ESPA system with a total gain of 6.75 dB in the vertical orientation.

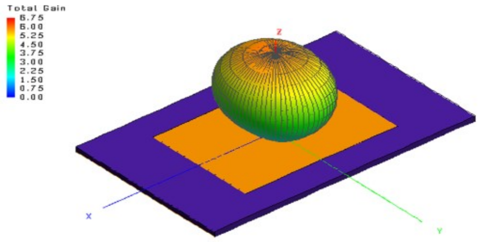

Fig. 10. Radiation Pattern of the ESPA System at 2.8 GHz

B. Performance Analysis of ESPA Configuration Orders

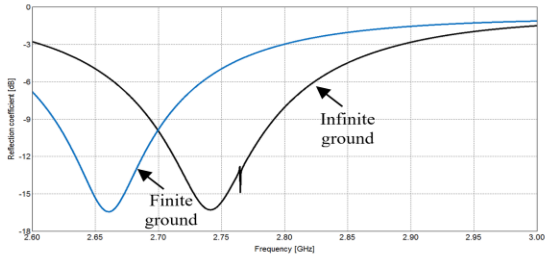

Fig. 11. Reflection Coefficient versus Frequency of Second Order ESPA

Fig. 11 give the reflection coefficient versus frequency for the second-order ESPA configuration. The second-order model resonates at about 2.66 GHz on the finite ground and 2.74 GHz on the infinite ground with a resonance difference of about 2.9%. Second-order model exhibits a 0.2% drop in its difference from the first-order ESPA with a frequency shift of almost 0.1 GHz. The simulated model with two ellipses generates the same reflection coefficient of -9.8 dB at 2.69 GHz. The characteristic impedance of 50 appears at the resonating frequency of 2.66 GHz on the finite ground. The VSWR values for the matched models of second-order configuration system is approximately 5.7 dB at 2.69 GHz. The radiation pattern of the second-order system is linearly polarized with a total gain of 6.0 dB at 2.8 GHz.

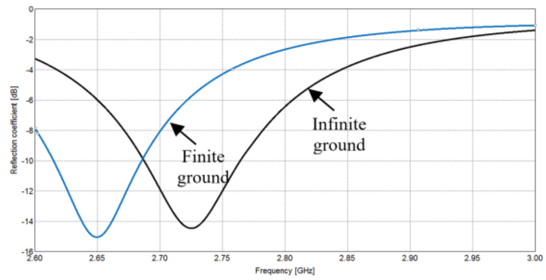

Fig. 12. Reflection Coefficient versus Frequency of Third-Order ESPA

Fig. 12 shows the frequency response in relation to the reflection coefficient of the third-order configuration. The resonating frequency of this model shifted away from the designing frequency to about 2.64 GHz with a reflection coefficient value of 15.05 dB on the finite ground. The resonating frequency of the third-order on the infinite ground is almost 2.72 GHz with a reflection coefficient value of -14.5 dB. The resonance frequency difference is further reduced by about 0.4% from the second-order configuration and which is approximately 2.5% in the third-order configuration. The models give the same reflection coefficient of about -9.8 dB at 2.68 GHz. Both second and third-order models show similar reflection coefficient values at the matched models with an approximate difference of about 2 dB from the basic ESPA model. The impedance magnitude with characteristic value is exhibiting on its resonant frequency with a 0.09 GHz from the first-order model. The VSWR values on the finite and infinite ground are 3.1 dB and 3.3 dB respectively. The radiation pattern shows a similar gain as that of the second-order ESPA system.

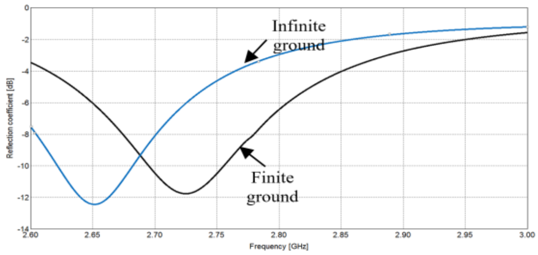

Fig. 13. Reflection Coefficient versus Frequency of Third-Order ESPA (Closer Approach)

Fig. 13 represents the frequency response of another third-order model with variations in the alignment of the ellipses as shown in Fig. 4. The system shows same resonance difference in both models with three ellipses irrespective of the location. However, there is a significant change in its reflection coefficient values compared with the prior model. The finite model resonates with a reflection coefficient value of 12.4 dB whereas; it is about -11.7dB for the infinite model with same value at -9.35 dB. The third-order model on the finite ground exhibited the characteristic 50 impedance at 2.66 GHz which is at about 0.13 GHz away from the designed frequency. This frequency shift attributed to the presence of more ellipses at the rectangular patch. The VSWR values corresponding to this design is about 4.23 dB on finite and infinite substrate.

The reflection coefficient versus frequency of the fourth-order configuration is in Fig. 14. The model with four ellipses on the finite ground resonates at 2.65 GHz and on the infinite ground resonates at 2.71 GHz. The resonance frequency difference reduced to 2.2% and which is about 0.9% drop from the first-order model. The fourth-order configuration also exhibits a characteristic impedance at their corresponding resonance frequencies. The VSWR for the closely-matched finite and infinite grounds is approximately 4.95 dB at a frequency of 2.68 GHz.

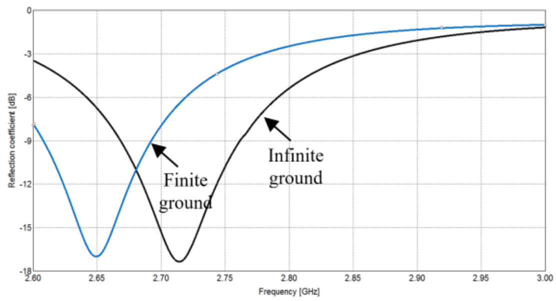

Fig. 14. Reflection Coefficient versus Frequency of Fourth-Order ESPA

The performance of second to fourth order configurations are summarized in Table II.

The first-order ESPA was designed to work on 2.79 GHz but it is resonant at 2.74 GHz. It is evident from the further order configurations that the resonant frequency shifts away from the design frequency. As the number of ellipses increases, the fringing fields around the antenna contributes towards the frequency shift. Fig. 15 shows the fabricated models corresponding to the FEKO models from first to fourth-order.

C. Performance of ESPA with Complex Dielectric Properties of Biosamples

The dielectric properties of biosamples can be introduced into the ESPA model by creating a cylindrical shape at the centre of the ellipse. The properties such as density, relative permittivity, loss tangent and conductivity are initiated into the cylinder at the centre of the ellipse to behave like a bio-sample for the simulation. Fig. 16 indicates the frequency response comparison of first-order ESPA on the finite ground and the ESPA with the properties of blood. The finite ESPA with a single ellipse resonates at 2.74 GHz and the model with blood properties resonates at 2.75 GHz with about -31.5 dB.

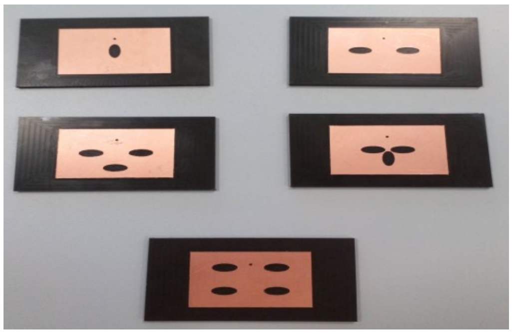

Fig. 15. Fabricated ESPA models

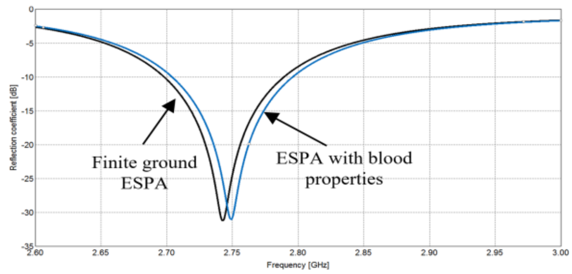

Fig. 16. Reflection Coefficient versus Frequency of ESPA and ESPA with properties of blood

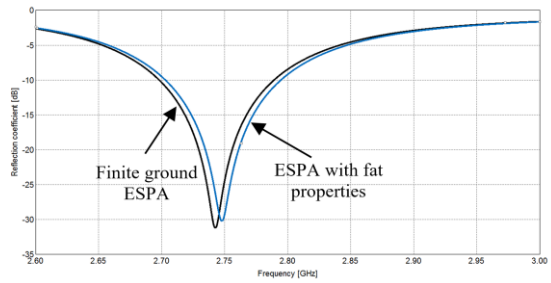

Fig. 17. Reflection Coefficient versus Frequency of ESPA and ESPA with properties of fat

Fig. 17 shows the reflection coefficient versus frequency for the basic ESPA system and the system with the dielectric properties of fat at the centre of the ellipse. The ESPA with fat resonates at about 2.74 GHz which is similar to the previous one but, with a significant variation in its reflection coefficient value of approximately -30 dB. The variation in the values of reflection coefficients are critical as this is responsible for detecting the changes in each bio-sample.

TABLE II PERFORMANCE SUMMARY OF ESPA CONFIGURATIONS

Performance Analysis Parameters	Second-Order	Third-Order	Fourth-Order
Resonating Frequency (GHz) Value (Finite Ground)	2.74	2.64	2.65
Resonant Frequency Difference (%)	2.9	2.5	2.2
Frequency at Characteristic Impedance (50)	2.66	2.65	2.65
VSWR (dB) value (finite ground)	3.2	3.1	2.4
Gain (dB)	6	6	6

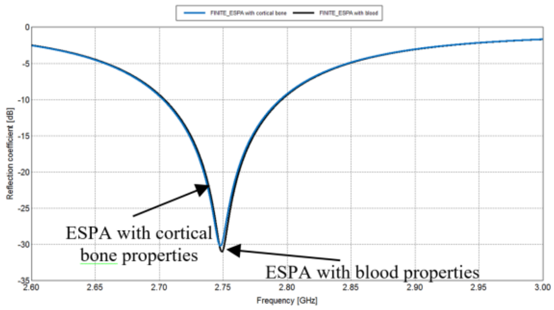

Fig. 18. Reflection Coefficient versus Frequency of ESPA with properties of blood and cortical bone

Unlike contrasting with the ESPA on finite ground, the frequency response of two biosamples such as blood and cortical bone with their dielectric properties are shown in Fig. 18.

IV. CONCLUSION

This paper presents the design of RF multi-band elliptically slotted patch antenna for bio-sensing applications. The introduced system yields a gain of 6.75 dBi with a 2:1 ratio on the semi-major to semi-minor axes. The proposed system is expanded to further order configurations with the insertion of more ellipses and exhibited a significant improvement in its resonance differences on finite and infinite grounds. The sensitivity of the system is tested using the dielectric properties of biosamples within the ellipse. The variations in the reflection coefficient corresponding to each sample promises the viability of the system in bio-sensing applications. The ESPA model is more appropriate for the real-time bio-sensing applications as the miniaturized size leads to easy fabrication with low cost and low profile. As consideration for future work, the ESPA model will be integrated into a reconfigurable architecture to investigate the effect of biosamples in the sub-6GHz 5G frequencies.

REFERENCES

[1] E. Kirshin, B. Oreshkin, G. K. Zhu, M. Popovic, and M. Coates, “Microwave Radar and Microwave-Induced Thermoacoustics: Dual-Modality Approach for Breast Cancer Detection,” IEEE Transactions on Biomedical Engineering, vol. 60, no. 2, pp. 354–360, Feb 2013.

[2] M. D. Hossain and A. S. Mohan, “Cancer Detection in Highly Dense Breasts Using Coherently Focused Time-Reversal Microwave Imaging,” IEEE Transactions on Computational Imaging, vol. 3, no. 4, pp. 928– 939, Dec 2017.

[3] N. Zarnaghi Naghsh, A. Ghorbani, and H. Amindavar, “Compressive sensing for microwave breast cancer imaging,” IET Signal Processing, vol. 12, no. 2, pp. 242–246, 2018.

[4] M. A. Aldhaeebi, T. S. Almoneef, H. Attia, and O. M. Ramahi, “NearField Microwave Loop Array Sensor for Breast Tumor Detection,” IEEE Sensors Journal, vol. 19, no. 24, pp. 11867–11872, Dec 2019.

[5] A. P. Gregory and R. N. Clarke, “A review of RF and microwave techniques for dielectric measurements on polar liquids,” IEEE Transactions on Dielectrics and Electrical Insulation, vol. 13, no. 4, pp. 727–743, Aug 2006.

[6] A. F. Mirza, C. H. See, I. M. Danjuma, R. Asif, R. A. Abd-Alhameed, J. M. Noras, R. W. Clarke, and P. S. Excell, “An Active Microwave Sensor for Near Field Imaging,” IEEE Sensors Journal, vol. 17, no. 9, pp. 2749–2757, May 2017.

[7] S. C. Ekpo, B. Adebisi, D. George, R. Kharel, and M. Uko, “System-level Multicriteria Modelling of Payload Operational Times for Communication Satellite Missions in LEO,” Recent Progress in Space Technology, vol. 4, no. 1, pp. 67–77, June 2014. [Online]. Available: http://www.eurekaselect.com/node/122892/article

[8] S. C. Ekpo, “Thermal Subsystem Operational Times Analysis for Ubiquitous Small Satellites Relay in

LEO," International Review of Aerospace Engineering (IREASE), vol. 11, no. 2, pp. 48–57, April 2018.

[9] S. C. Ekpo, "Parametric System Engineering Analysis of CapabilityBased Small Satellite Missions," IEEE Syst. J., pp. 3546–3555, September 2019.

[10] S. C. Ekpo, V. Velusamy, and R. Kharel, "A Novel Elliptically-Slotted Patch Antenna-based Biosensor Design," 2015.

[11] S. C. Ekpo and D. George, "Impact of Noise Figure on a Satellite Link Performance," IEEE Commun. Lett., vol. 15, no. 9, pp. 977–979, September 2011.

[12] S. C. Ekpo, B. Adebisi, and A. Wells, "Regulated-Element Frost Beamformer for Vehicular Multimedia Sound Enhancement and Noise Reduction Applications," IEEE Access, vol. 5, pp. 27254–27262, Dec 2017.

[13] M. Uko and S. Ekpo, "8-12 GHz pHEMT MMIC Low-Noise Amplifier for Fiber-Integrated Satellite Applications," International Review of Aerospace Engineering (IREASE), pp. 1–10, February 2020.